

Electronic Supplementary Information:

Gold nanoplates with superb photothermal efficiency and peroxidase-like activity for rapid and synergistic antibacterial therapy

Lu Yan ^{a,1}, Jie Mu ^{a,1}, Pengxin Ma ^{a,1}, Qian Li ^b, Pengxue Yin^a, Xuan Liu^a, Yuanyuan Cai^a,
Haipeng Yu^a, Junchong Liu^a, Guoqing Wang^b, and Aihua Liu^{a*}

^aInstitute for Chemical Biology & Biosensing, and College of Life Sciences, School of Pharmacy, Medical College, Qingdao University, 308 Ningxia Road, Qingdao 266071, China

^b College of Food Science & Engineering, Ocean University of China, 5 Yushan Road, Qingdao 266003, China

¹These authors contributed equally to this work.

*Corresponding author. E-mail address: liuah@qdu.ac.cn (A. Liu).

Table of contents:

- 1. Experimental**
- 2. Supplementary scheme and figures**

1. Experimental

1.1 Materials and methods

1.1.1. Chemicals and materials

3-(4,5-Dimethylthiazol-2-yl)-2,5-diphenyltetrazoliumbromide (MTT), polyvinylpyrrolidone K30 (PVP-K30), sodium borohydride, Luria-Bertani (LB) medium, chloroauric acid and hydrogen peroxide (H_2O_2 , 30%) were purchased from Sinopharm Chemical Reagent Co. (Shanghai, China). Propidium iodide (PI) and 4,6-diamidino-2-phenylindole (DAPI) were purchased from Solarbio Reagent Co. (Shanghai, China). 3,3',5,5'-Tetramethylbenzidine (TMB) was purchased from TCI Development Co. (Shanghai, China). Sodium azide (NaN_3) was obtained from Sigma-Aldrich (St. Louis, USA). The 96-well microtiter plate was purchased from Nunc (Thermo Fisher Scientific Co., Ltd., Denmark). *Bacillus Cereus* (*B. Cereus*), *Escherichia coli* Trans 5 α (*E. coli* Trans 5 α), *Edwardsiella tarda* (*E. tarda*), *Proteus vulgaris* (*P. vulgaris*), *Escherichia coli* K91BK (*E. coli* K91BK), *Staphylococcus aureus* (*S. aureus*), MRSA and tetracycline-resistant *Escherichia coli* K12 (*E. coli* K12) are available in our laboratory.

1.1.2. Preparation of AuNPTs

The AuNPTs was synthesized based on a previously reported method¹ preposed by our coauthor with minor modification. Briefly, HAuCl_4 (10 mM, 1 mL) and trisodium citrate (10 mM, 0.2 mL) were added into 18.5 mL of pure water. Followed by NaBH_4 (0.1 M, 0.5 mL) was added under vigorous stirring for 5 min. Then the seed solution was left for aging for over 3 h. In the growth step, HAuCl_4 (10 mM, 7 mL) and PVP-K30 (2 mM, 14 mL) were mixed with 133 mL of pure water under sonication, to which 1.4 mL of the above seed solution was injected. Finally, 15 μL H_2O_2 (30 wt%) was introduced to trigger the seeded growth of AuNPTs, which was incubated at room temperature for 3 h. Finally, the resultant solution was centrifuged twice, 10000 rpm for 5 min, 5000 rpm for 5 min, and resuspended in 6 mL water to obtain a suspension of AuNPTs.

Note: The addition of H_2O_2 during the synthesis of gold nanoplates tended to grow into plates rather than other shapes¹. The extinction spectra exhibiting typical local surface plasmon resonance (LSPR) spectra, in which the transverse peak located around 530 nm

while the longitudinal peak located ranging from 700 nm to 900 nm, depending on the dosage of H₂O₂ as the initiator (Fig. S2A). As H₂O₂ concentration increased, the longitudinal peak gradually shifted blue, which was similar to that reported previously¹. When H₂O₂ (30 wt%) dosage increased to 15 μL, the longitudinal peak of the AuNPTs appeared at 805 nm, which is the similar wavelength for that value of the 808-type NIR laser, suggesting that the highest photothermal conversion efficiency can be obtained^{2, 3}. Therefore, 15 μL of H₂O₂ (30 wt%) was used for subsequent synthesis. The extinction spectra of three batches of gold nanoplates are almost identical (Fig.S2B), indicating that the synthesis had good reproducibility. Fig.S2C compares the extinction spectra of the AuNPTs before and after purification by twice centrifugation. After centrifugation two times, the transverse peak for the gold nanoplates was significantly reduced compared to the case of non-purification, indicating that most gold nanospheres could be removed by centrifugation.

1.2. Instrumentation

The vis–NIR absorption spectra were recorded with U-2910 spectrophotometer (Hitachi, Japan). The absorbance was measured with a SPARK 10 M multi-function microplate reader (Tecan, Switzerland). Transmission electron microscopy (TEM) images were taken on a FEI F20 S-TWIN instrument (Thermo Scientific, USA). The Zeta potential of the prepared materials was measured at 25 °C by Zetasizer Nano ZSP (Malvern, UK). The NIR light was excited by the infrared laser T808D1W (Xi'an Minghui Optoelectronics, China). The thermal images were taken by the thermal camera FLIR E50 (Shenzhen Jiexin Electric, China). Fluorescent pictures were taken with an inverted fluorescence microscope IX71 (Olympus, Japan). The morphology of the bacteria was observed on a JEM-2010 transmission electron microscope (JEOL Ltd., Japan).

1.3. Characterization of peroxidase-like activity of AuNPTs

To determine the peroxidase-like activity, AuNPTs (50 μg/mL), TMB (0.5 mM) and H₂O₂ (0.5 mM) were added in PBS solution (pH 6.0) and incubated at room temperature for 30 min. The absorption spectrum within 400–800 nm was recorded with a spectrophotometer.

1.4. Photothermal effect of AuNPTs

First, the effect of AuNPTs dosage on the photothermal property was studied by applying

AuNPTs at different concentrations (0, 10, 20, 30, 50, 100, 150 $\mu\text{g}/\text{mL}$) under irradiation with an 808 nm NIR laser ($1 \text{ W}/\text{cm}^2$, 5 min). Then, in order to measure the temperature change under different laser power densities, the experiment was carried out by using AuNPTs with a concentration of 20 $\mu\text{g}/\text{mL}$. Lastly, the photothermal conversion efficiency of AuNPTs was calculated according to the literature⁴. AuNPTs (20 $\mu\text{g}/\text{mL}$, 1 mL) was irradiated by a laser power density ($1 \text{ W}/\text{cm}^2$) for 10 min and then cooled down gradually at room temperature to reach the equilibrium temperature. The temperature was recorded every 30s.

1.5. In vitro antibacterial experiment

1.5.1 In vitro cytotoxicity testing

L929 cells were kindly gifted by Dr Yuanhong Xu in our institute, which were cultured in a 96-well plate at a density of 10^4 cells per well for 24 h and then incubated with AuNPTs with different concentrations (0, 15, 25, 50, 100, 200 $\mu\text{g}/\text{mL}$) for 24 h. After that, the cell survival rates were detected using the standard MTT assay.

1.5.2 Bacterial culture

First, single colonies of *E. coli* K12 and MRSA on solid Luria-Bertani (LB) agar plates were transferred to 5 mL liquid LB medium in the presence of tetracycline ampicillin (200 $\mu\text{g}/\text{mL}$) at 37 °C to grow for 12 h. Then, the bacteria in the LB medium were centrifuged and resuspended in the same volume of phosphate buffer saline (PBS). Finally, the absorbance at 600 nm ($\text{OD}_{600 \text{ nm}}$) of the suspension was adjusted to about 0.1, for which the bacterial concentration was about 10^6 CFU/mL (CFU, colony-forming unit). The obtained bacterial suspension was used in the subsequent experiment.

1.5.3 Antibacterial experiment based on peroxidase-like activity of the AuNPTs

Bacteria were incubated with 50 $\mu\text{g}/\text{mL}$ AuNPTs mixing with different concentrations of H_2O_2 (0, 0.1, 0.5, 1 mM) buffered with PBS (pH 6.0) for 30 min at 37 °C. Then, the diluted bacterial suspension (50 μL) was transferred into LB agar plates and incubated at 37 °C for 24 h. The number of colonies were counted. Finally, to further explore its antibacterial effect, the growth curves of two bacteria were studied. Bacteria were cultured in LB medium with different treatments. All groups were incubated at 37 °C for 11 h and the $\text{OD}_{600 \text{ nm}}$ values were measured using a microplate reader.

1.5.4 Antibacterial experiment based on photothermal effect

The bacterial suspension was mixed with different concentrations of AuNPTs solution (0, 4, 10, 20, 30, 50, 100 $\mu\text{g/mL}$) with a final volume of 200 μL in a 96-well plate under NIR light (808 nm, 1 W/cm^2 , 5 min). The temperature change after heating for 5 min was monitored. Standard plating methods were used to determine bacterial survival. The effect of laser power density on the survival of the bacteria was measured with 50 $\mu\text{g/mL}$ AuNPTs solution for 5 min. After the treatment, the solution was diluted to an appropriate multiple, then incubated on agar plates at 37 $^{\circ}\text{C}$ for 24 h for CFU counting.

1.5.5 Synergistic antibacterial experiment based on catalysis of peroxidase-like and photothermal property

Two bacteria were treated with different groups, PBS (pH 6), AuNPTs (50 $\mu\text{g/mL}$), AuNPTs (50 $\mu\text{g/mL}$)/ H_2O_2 (0.1 mM), AuNPTs (50 $\mu\text{g/mL}$)/NIR (1 W/cm^2 , 3 min) and AuNPTs (50 $\mu\text{g/mL}$)/ H_2O_2 (0.1 mM)/NIR (1 W/cm^2 , 3 min). Herein NIR indicates 808 nm laser light illumination. The temperature change was monitored after 3 min and the bacterial survival was obtained by plate counting.

Single strains or strains mixture were tested the universality of the combination sterilization of photothermal and hydrogen peroxide with AuNPTs (50 $\mu\text{g/mL}$)/ H_2O_2 (0.1 mM)/NIR (1 W/cm^2 , 3 min). The bacterial survival was obtained by plate counting.

1.5.6 Live/dead cell fluorescent staining

The live/dead bacteria were fluorescently stained with DAPI and PI. After treatment with AuNPTs (50 $\mu\text{g/mL}$, pH 6)/ H_2O_2 (0.1 mM)/NIR (1 W/cm^2 , 3 min), both MRSA and *E. coli* K12 bacteria were harvested by centrifugation and stained for 15 min at ambient temperature in the darkness.

1.6. In vivo antibacterial experiments

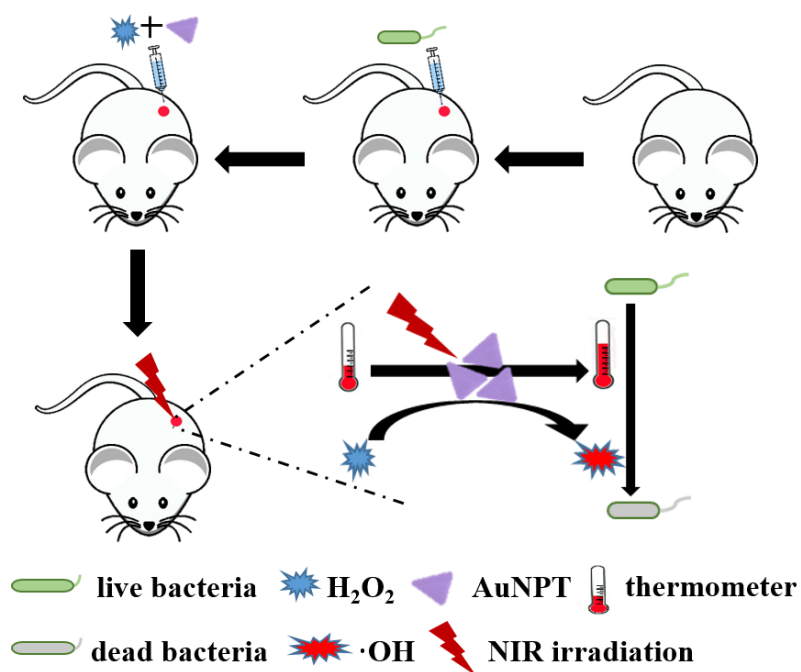
~150 g healthy Sprague-Dawley (SD) rats were randomly classified into six groups (8 mice each group). Considering that multiple skin wounds on one rat may cause interference each other, one skin wound on one mouse was applied. After anesthesia, a circular full-thickness skin wound of approximately 6 mm in diameter was formed on the right thigh

surface of the mouse with a punch. Then 10 μL of 1×10^7 MRSA cells suspension was inoculated the wounds. The mice were raised under normal conditions with different treatments only in the first day. Then the wounds were exposed without any additional disinfection methods used during the following days of treatments. The wounds were recorded and photographed every two days. After two days, the wound tissues were harvested from three random mice in each group. To determine the number of bacteria, the wound tissues were placed in 1 mL PBS and homogenized and incubated overnight at 37 $^{\circ}\text{C}$. Then, the suspensions were diluted by appropriate multiples and grown on agar plates at 37 $^{\circ}\text{C}$ for 24 h. Finally, the number of bacterial colonies were counted. Animal studies were conducted in compliance with the guidelines of the Institutional Animal Care and Use Committee, Institutional Review Board, Affiliated Hospital of Qingdao University.

Histology: After six days, different groups of wound tissue from the left 5 mice were harvested. Then, fixed in 10 % paraformaldehyde, embedded in paraffin and cut into slices of about 4 μm . The tissue samples were examined under a fluorescence microscopy after stained with hematoxylin-eosin staining (H&E).

In vivo biosafety: AuNPTs (200 $\mu\text{g}/\text{mL}$) were subcutaneously injected into healthy mice with each group having 3 mice. After 6 days' feeding, the main organs were collected from mice treated with AuNPTs or PBS for pathological examination. Blood samples for blood biochemical examination were collected from the mice on the sixth day.

2. Supplementary Scheme and figures



Scheme S1 Schematic diagram of antibacterial and wound-curing to mouse surface wounds with AuNPTs based peroxidase-like activity and superb photothermal property.

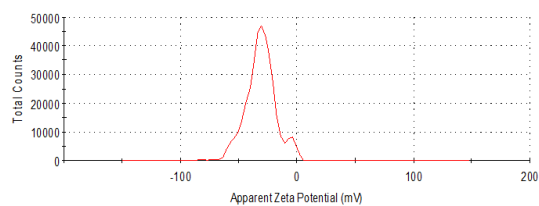


Fig.S1 Profile of apparent Zeta potential of the as-prepared AuNPTs

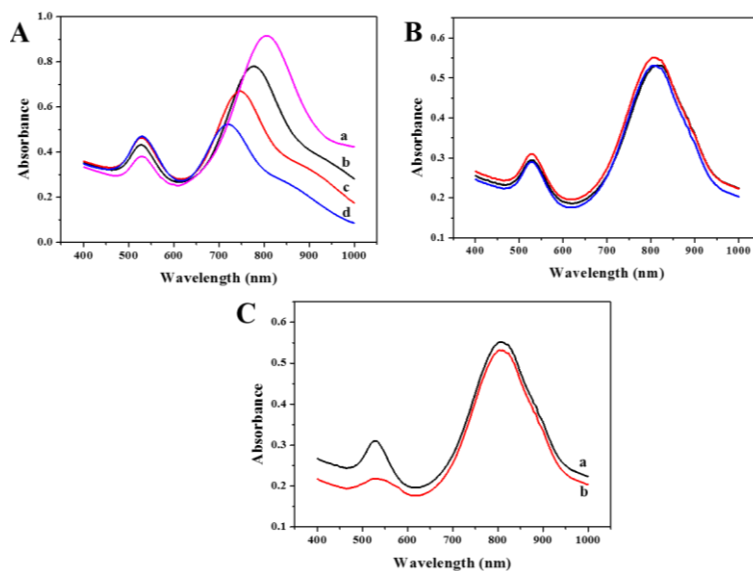


Fig.S2 (A) Extinction spectra of AuNPTs synthesized with varying H_2O_2 dosage (a-d: 15, 20, 25, 30 μL). (B) Extinction spectra of three batches of AuNPTs prepared with the same conditions. (C) Extinction spectra of the AuNPTs (a, as-prepared; b, after twice centrifugation).

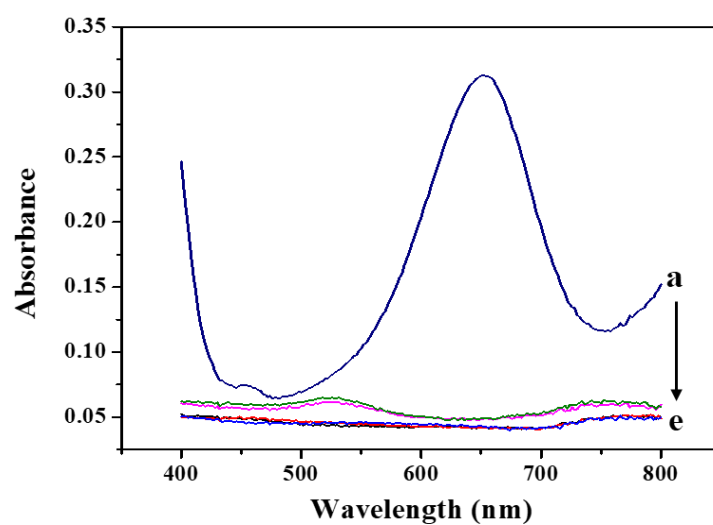


Fig.S3 Vis-NIR absorption spectra of different solutions. a, AuNPTs ($50 \mu\text{g mL}^{-1}$)/TMB (0.5 mM)/ H_2O_2 (0.5 mM)/PBS (pH 6.0); b, AuNPTs ($50 \mu\text{g mL}^{-1}$); c, TMB (0.5 mM)/ H_2O_2 (0.5 mM); d, AuNPTs ($50 \mu\text{g mL}^{-1}$)/TMB (0.5 mM); e, AuNPTs ($50 \mu\text{g mL}^{-1}$)/ H_2O_2 (0.5 mM). All these groups are incubated at $25 \text{ }^\circ\text{C}$ for 30 min.

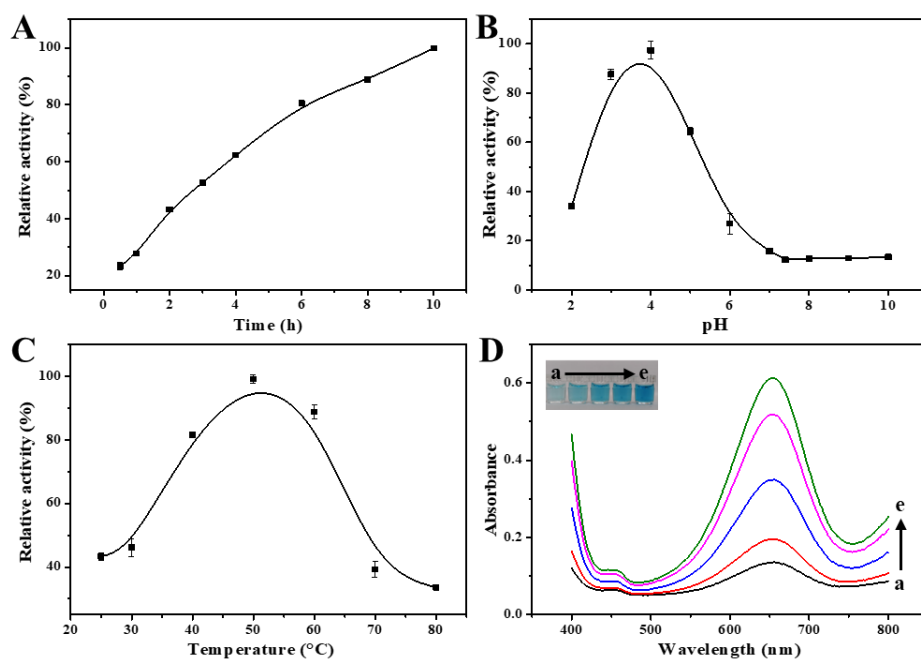


Fig.S4 Optimization of the peroxidase-like activity of AuNPTs. For each curve, the highest point is defined as 100 % relative enzyme activity. (A) Effect of incubation time on the catalytic performance of AuNPTs. H_2O_2 (0.5 mM)/TMB (0.5 mM)/AuNPTs (50 $\mu\text{g}/\text{mL}$) buffered with PBS (pH 6) incubated at 25 $^\circ\text{C}$ for different time. (B) Effect of solution pH on the catalytic performance of AuNPTs. H_2O_2 (0.5 mM)/TMB (0.5 mM)/AuNPTs (50 $\mu\text{g}/\text{mL}$) with varying buffer pH incubated at 25 $^\circ\text{C}$ for 30 min. (C) Effect of temperature on the catalytic performance of AuNPTs. H_2O_2 (0.5 mM)/TMB (0.5 mM)/AuNPTs (50 $\mu\text{g}/\text{mL}$) buffered with PBS (pH 6) incubated for 30 min varying temperature. (D) Vis-NIR spectra of solutions. H_2O_2 (0.5 mM)/TMB (0.5 mM) buffered with PBS (pH 6) incubated with varying AuNPTs concentrations at 25 $^\circ\text{C}$ for 30 min. AuNPTs concentration for curves a–e: 10, 25, 50, 100, 150 $\mu\text{g}/\text{mL}$. In all the above cases, the incubation solutions were centrifuged before spectra or absorbance measurements.

Note: The optimum peroxidase-like activity is exhibited at pH 4.0, and 25% of the maximal catalytic activity can be retained around pH 6.0 (Fig.S4B). The normal pH range of skin is within 4.8 to 6⁵, which is mainly caused by skin cutin. When the wound is infected with bacteria, its acidity may increase further due to acute inflammation. On the other hand, the enzyme activity increased with increasing temperature and reached a plateau at 50 $^\circ\text{C}$, thereafter the the enzyme activity decreased (Fig. S4C). However, 88% of the maximal catalytic activity can be maintained at 60 $^\circ\text{C}$ (Fig.S4C).

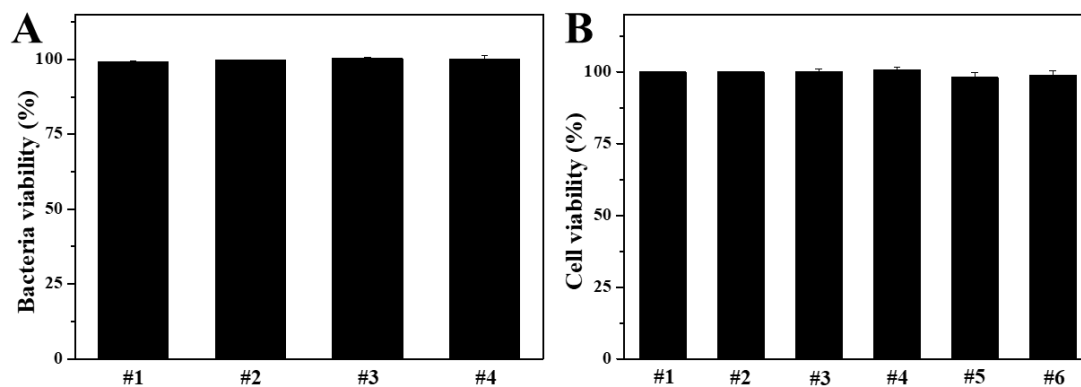


Fig.S5 (A) Survival rates of different bacteria incubated in culture media with 200 µg/mL AuNPTs in PBS (pH 6.0) for 2h. Bacteria speices: #1, *E. coli* Trans 5α; #2, *E. tarda*; #3, *E. coli* K91BK; #4, *S. aureus*. (B) Cytotoxicity of AuNPTs at different concentrations. AuNPTs concentration: #1–#6: 0, 15, 25, 50, 100, 200 µg/mL.

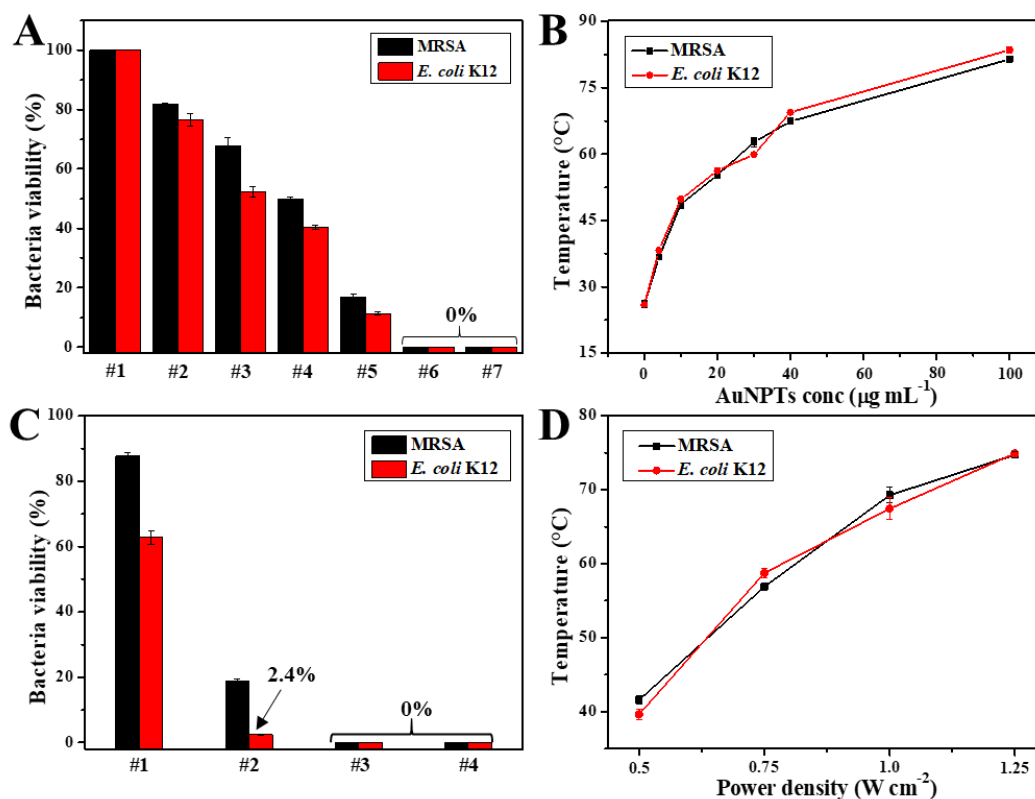


Fig.S6 (A) Bacterial viability of MRSA and *E. coli* K12 incubated with varying AuNPTs concentrations under 808 nm laser irradiation (1 W/cm², 5 min). AuNPTs concentration for #1–#7: 0, 4, 10, 20, 30, 50, 100 μg/mL. (B) The temperature of bacterial suspension as a function of AuNPTs concentrations under 808 nm laser irradiation (1 W/cm², 5 min). (C) Bacterial viability of MRSA and *E. coli* K12 incubated with 50 μg/mL AuNPTs under 808 nm laser irradiation for 5 min varying with laser power density. Power densities for #1–#4: 0.5, 0.75, 1, 1.25 W/cm². (D) The temperature of bacterial suspension as a function of laser power density under NIR laser irradiation (808 nm laser, 5 min).

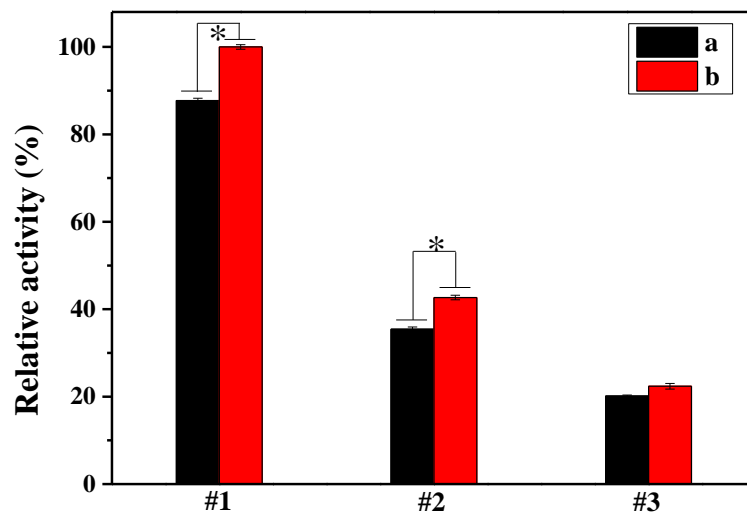


Fig.S7 Effect of 808 nm laser irradiation on the peroxidase-like activity of AuNPTs. The AuNPTs (50 $\mu\text{g/mL}$) solutions were initially treated without NIR irradiation (a) or with NIR irradiation (b) (808 nm laser, 2 W/cm^2 , 5 min), which were further incubated with H_2O_2 (0.5 mM)/TMB (0.5 mM) with varying buffer pHs at 25 $^\circ\text{C}$ for 30 min. The incubation solutions were centrifuged before absorbance measurements. Buffer solution pH: #1, pH 4.0; #2, pH 6.0; #3, pH 7.0.

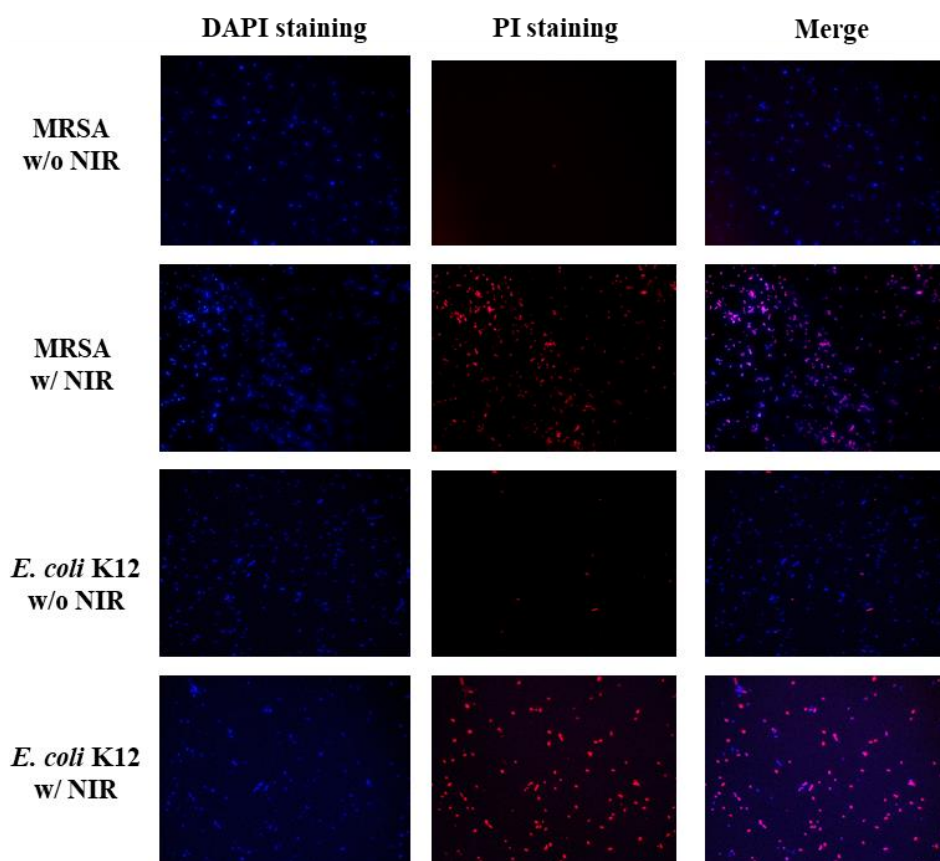


Fig.S8 Typical fluorescence images of live and dead MRSA/*E. coli* K12 cells after various treatments with AuNPTs ($50 \mu\text{g mL}^{-1}$)/ H_2O_2 (0.1 mM), AuNPTs ($50 \mu\text{g mL}^{-1}$)/ H_2O_2 (0.1 mM)/NIR irradiation (808 nm, 1 W cm^{-2} , 3 min). 4,6-diamidino-2-phenylindole (DAPI) staining (blue) for all bacteria, Propidium iodide (PI) staining (red) for dead bacteria.

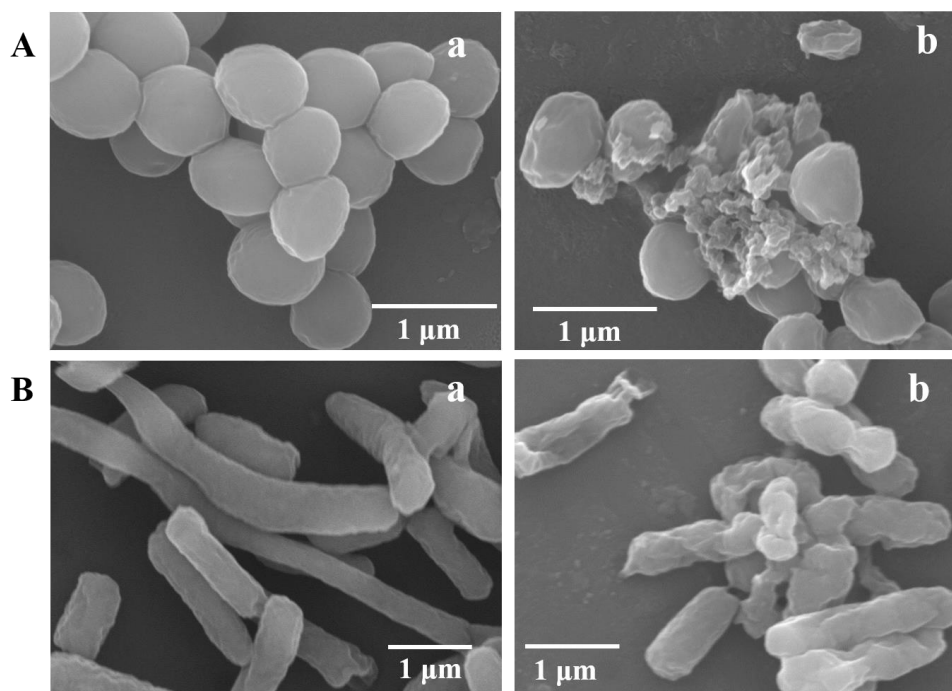


Fig.S9 Typical SEM images of (A) MRSA and (B) *E. coli* K12 cells with different treatments. (a) PBS, (b) AuNPTs (50 μg mL⁻¹)/H₂O₂ (0.1 mM)/NIR irradiation (808 nm, 1 W cm⁻², 3 min).

Note: Observed from SEM images, the untreated MRSA or *E. coli* K12 cells exhibited spherical- or rod-like shape, respectively. After NIR photoirradiation with AuNPTs (50 μg mL⁻¹)/H₂O₂ (0.1 mM), both of intact cell surfaces turned to severely rough and damaged. These results were corresponded to bacterial live/dead staining assay, indicating that NIR photothermal therapy assisted peroxidase-like catalysis has excellent synergistic antibacterial ability against MRSA or *E. coli* K12 cells.

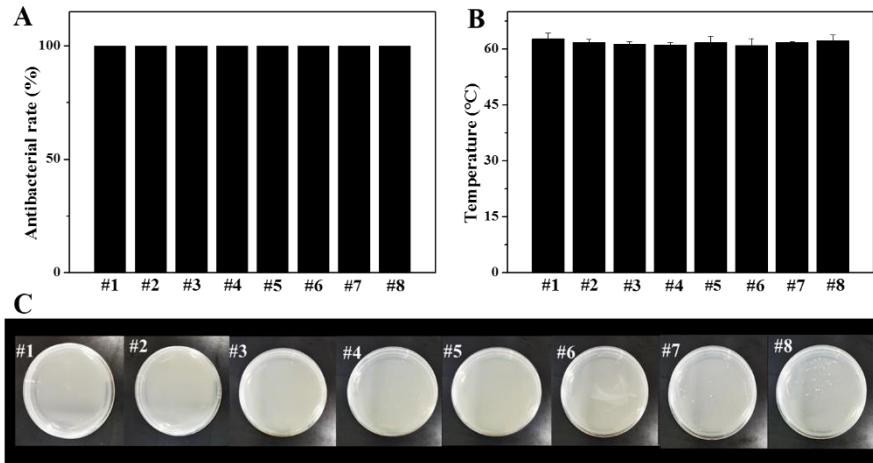


Fig.S10 (A) Bacterial viability of various bacterial colonies, which were treated with AuNPTs (50 $\mu\text{g/mL}$)/ H_2O_2 (0.1 mM)/NIR light irradiation (808 nm, 1 W/cm^2 , 3 min). (B) The temperature of various bacterial suspension in the presence of AuNPT (50 $\mu\text{g/mL}$)/ H_2O_2 (0.1 mM)/NIR light irradiation (808 nm, 1 W/cm^2 , 3 min). Strains: #1, *B. Cereus*; #2, *E. coli* Trans 5 α ; #3, *E. tarda*; #4, *P. vulgaris*; #5, *E. coli* K91BK; #6, *S. aureus*; #7, mixture of *B. Cereus*/*E. tarda*/*S. aureus*; #8, mixture of *B. Cereus*/*E. tarda*/*S. aureus*/*E. coli* Trans 5 α /*E. coli* K91BK. (C) Photographs of plates cultured with various bacterial colonies. The plates in the absence or in the presence of AuNPTs (50 $\mu\text{g/mL}$)/ H_2O_2 (0.1 mM)/NIR light irradiation (808 nm, 1 W/cm^2 , 3 min).

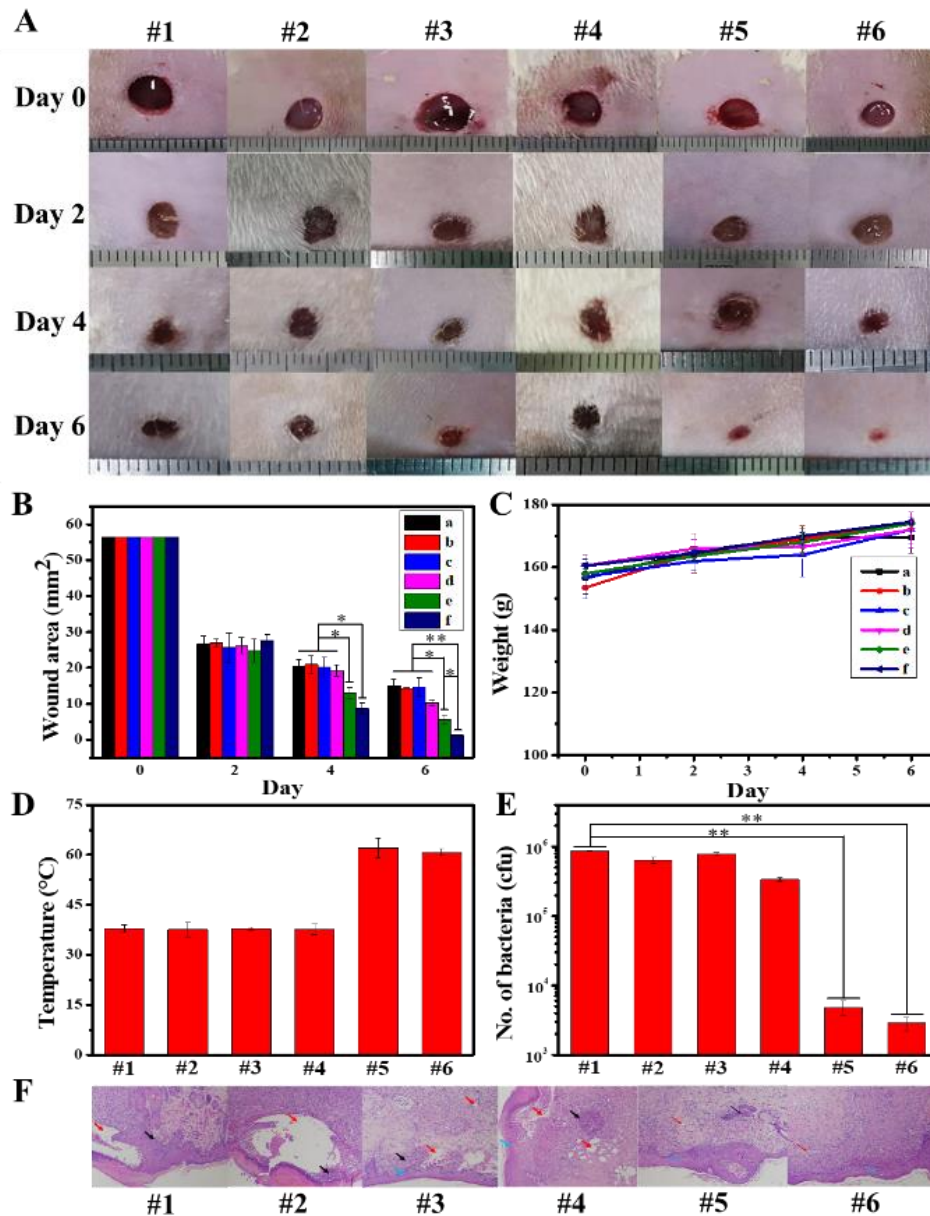


Fig.S11 Healing effect on the wound infected with MRSA. (A) Photographs of wounds on the right thigh of the rats after different treatments. The minimum scale of the rule, 1 mm. (B) The size of the wound area at different times. (C) Changes in body weight of mice in each experimental group within 6 days. (D) Maximum temperature of the wounds of rats in each experimental group during infrared irradiation. (E) The number of bacteria obtained from wound tissues after different treatments on Day 2. Error bars represent the standard deviation (n=3). Asterisks indicated statistically significant differences (*p < 0.05, **p < 0.01). (F) Histological data of corresponding skin wounds after different treatments (Black, blue, red arrows indicate inflammatory cells, epithelial cells, inter-tissue faults, separately). Treatment conditions: #1, PBS; #2, H₂O₂ (0.1 mM); #3, AuNPTs (50 μg mL⁻¹); #4, AuNPTs (50 μg mL⁻¹)/H₂O₂ (0.1 mM); #5, AuNPTs (50 μg mL⁻¹)/NIR (1 W cm⁻²); #6, AuNPTs (50 μg mL⁻¹)/H₂O₂ (0.1 mM)/NIR (1 W cm⁻²).

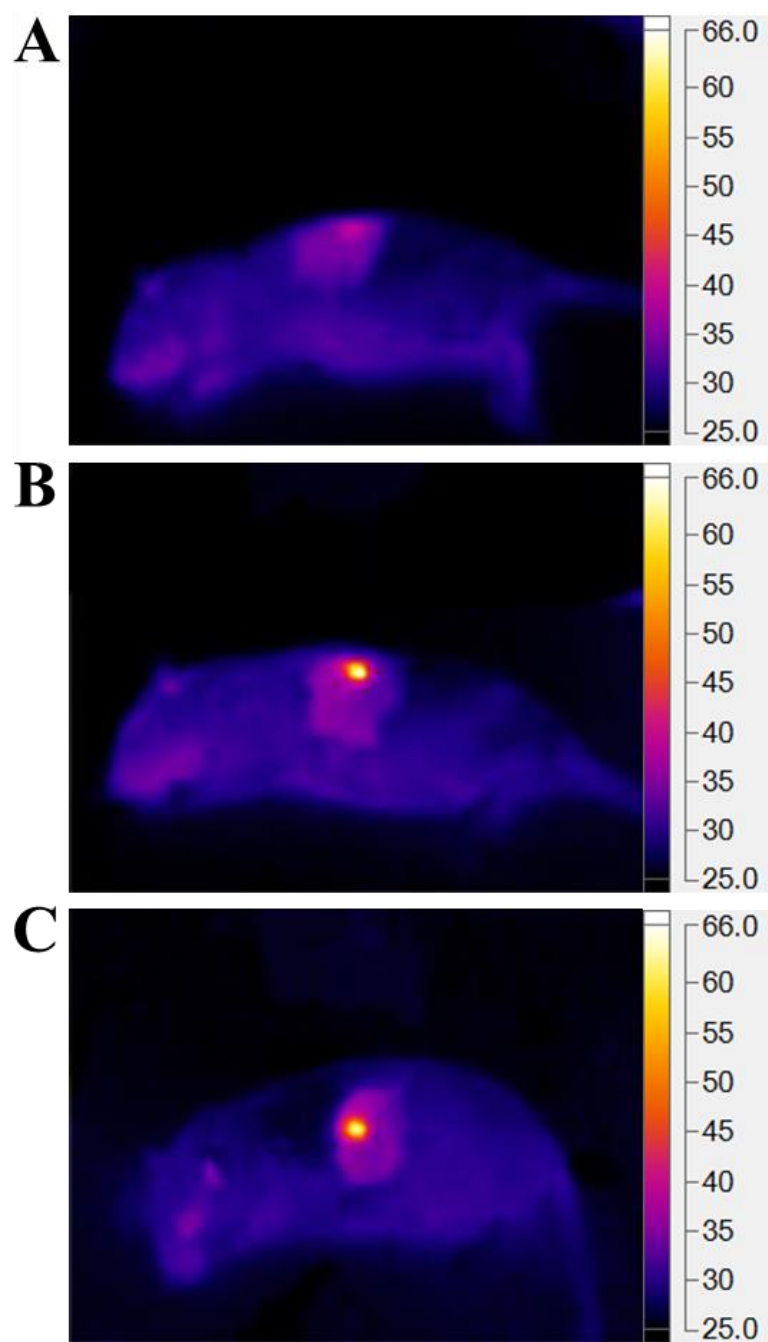


Fig.S12 Thermal images of mice surface after incubation with different medium. The pictures were taken after NIR irradiation. Culture media: (A), PBS/NIR (808 nm laser, 1 W/cm², 3 min); (B), AuNPTs (50 μg/mL)/NIR (808 nm laser, 1 W/cm², 3 min); (C), AuNPTs (50 μg/mL)/H₂O₂ (0.1 mM)/NIR (808 nm, 1 W/cm², 3 min).

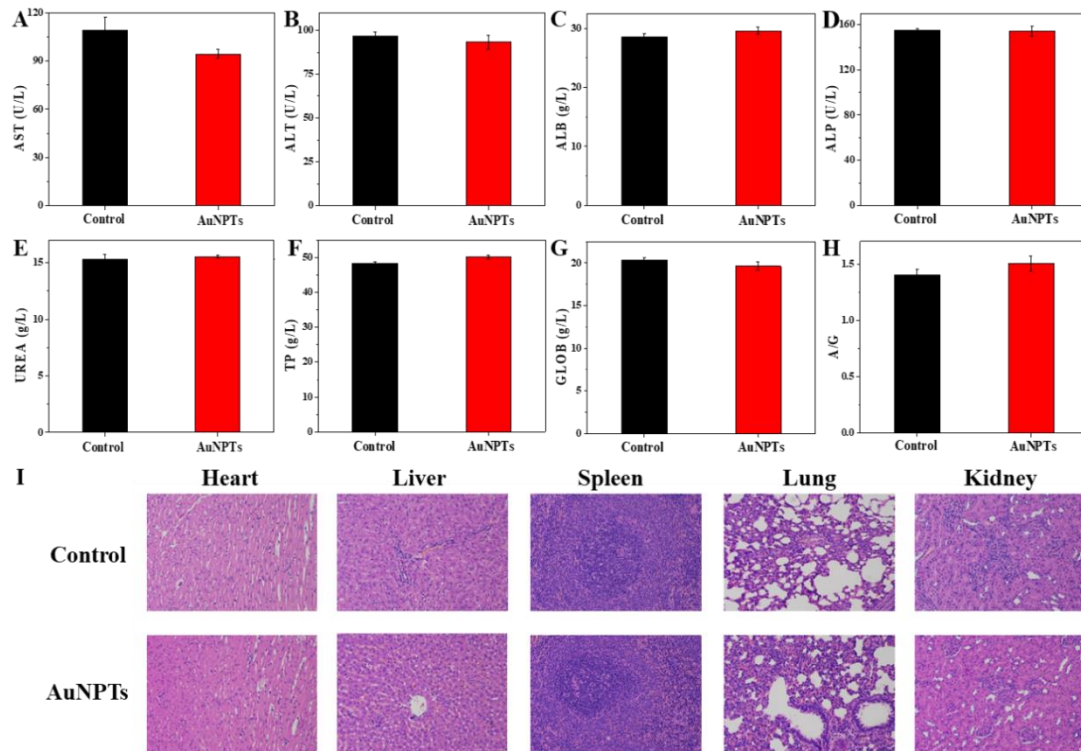


Fig.S13 Blood physiological indexes including (A) alkaline aspartate transaminase (AST), (B) alanine transaminase (ALT), (C) albumin (ALB), (D) phosphatase (ALP), (E) urea nitrogen (UREA), (F) total protein (TP), (G) globulin (GLOB) and (H) the ratio of albumin to globulin (A/G) of rats treated with 200 $\mu\text{g}/\text{mL}$ AuNPTs or the PBS (pH 6.0). Error bars represent the standard deviation ($n=3$). (I) Histological data of the major organs of rats treated with 200 $\mu\text{g}/\text{mL}$ AuNPTs or the PBS (pH 6.0). Blood samples and organ samples were collected from the mice on the sixth day.

References

1. G. Q. Wang, S. Y. Tao, Y. D. Liu, L. Guo, G. H. Qin, K. Ijiro, M. Maeda and Y. D. Yin, *Chem. Commun.*, 2016, **52**, 398-401.
2. J. Tang, X. Jiang, L. Wang, H. Zhang, Z. Hu, Y. Liu, X. Wu and C. Chen, *Nanoscale*, 2014, **6**, 3670-3678.
3. B. Hu, N. Wang, L. Han, M. L. Chen and J. H. Wang, *Acta Biomater.*, 2015, **11**, 511-519.
4. W. Z. Ren, Y. Yan, L. Y. Zeng, Z. Z. Shi, A. Gong, P. Schaaf, D. Wang, J. S. Zhao, B. B. Zou, H. S. Yu, G. Chen, E. M. B. Brown and A. G. Wu, *Adv. Healthc. Mater.*, 2015, **4**, 1526-1536.
5. A. Scalise, A. Bianchi, C. Tartaglione, E. Bolletta, M. Pierangeli, M. Torresetti, M. Marazzi and G. Di Benedetto, *Semin. Vasc. Surg.*, 2015, **28**, 151-159.